

Weno Scheme for Transport Equation on Unstructured Grids with a DDFV Approach

Florence Hubert and Rémi Tesson

Abstract In this paper we develop a DDFV approach for WENO scheme on unstructured grids for 2D transport equations. An order 2 scheme is presented using the DDFV diamond structure to define the different stencils. Numerical tests illustrate the accuracy and robustness of the method.

Keywords Weighted essentially non-oscillatory · Transport equation · Discrete duality finite volume scheme

MSC (2010): 65M08 · 65Z12 · 65D05

1 Introduction

The problems we are interested in are fluid-structure interaction problems in 2D, where we use a level-set approach. In such problems, we look at the behavior and displacement of a structure, that can be a solid or an elastic membrane, inside a fluid. The level-set approach consists, in this situation, in representing the interface between the fluid and the structure implicitly as the level-set of a function ϕ . The modelization of this situations often implies fluid mechanics equations, such as Stokes equations, coupled with transport equations.

Here we focus on numerical tools for the resolution of transport equations. Because the level-set function ϕ that captures the interface is the solution of a transport equation we want to be very sharp when solving this equation. Order one schemes are known to be very diffusive and inadapted in the level-set context. High order method, like WENO schemes, appear to be a good solution to solve precisely trans-

F. Hubert (✉) · R. Tesson (✉)
I2M, Marseille, 39 Rue F. Joliot Curie, 13453 Marseille, France
e-mail: florence.hubert@univ-amu.fr

R. Tesson
e-mail: remi.tesson@univ-amu.fr

port equation. First introduced by Harten, Osher and others [6–8, 13], WENO schemes are known to be efficient on convection problems.

The interest to use locally refined meshes is that it allows us to be accurate near the interface between fluid and structure although to be efficient in terms of computational time and memory. In this paper, we will develop a DDFV approach for WENO scheme on locally refined grids. The Discrete Duality Finite Volume method (DDFV) is a Finite Volume method, that has been successfully used to solve Stokes equations [11] on various kinds of meshes, including locally refined meshes. In Sect. 2 we will present the time and spatial discretization of the transport equation, in Sect. 3 we will expose the reconstruction procedure used in the WENO scheme in itself and then we will illustrate our statement with numerical tests in Sect. 4.

2 Discretization of the Transport Equation

2.1 Notations and DDFV Structure

In fluid-structure interaction problems, the velocity used in the transport equation is often given by fluid mechanics equations like Stokes equations. In such models we must couple the resolution of Stokes equations with the resolution of transport equation. In order to be able to deal with a large class of meshes and to release us from the orthogonality constraint imposed by VF4 methods (see [4]), we choose to use a DDFV strategy.

DDFV are Finite Volume methods introduced first in [3, 9]. They consist in a decomposition of the computing domain in a set of polygons. Those polygons form the primal mesh and one unknown is associated to the barycenter of each polygon. Then other unknowns are added on the vertices of the polygons. Those vertices are therefore seen as centers of other polygons that define a dual mesh as in Fig. 1. The interest of introducing new unknowns is that it allows us to compute an approximation of the gradient in every directions.

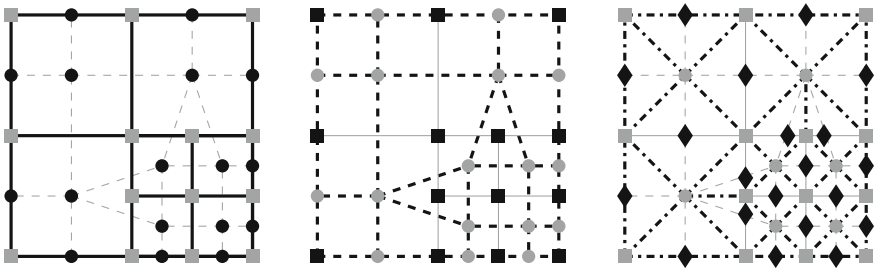


Fig. 1 DDFV structure. From the *left* to the *right* primal mesh, dual mesh and diamond structure

We denote by K a polygon of the primal mesh \mathfrak{M} and K^* a polygon of the dual mesh \mathfrak{M}^* . In the following, we will denote an element of the primal or dual mesh by $C \in \mathfrak{M} \cup \mathfrak{M}^*$.

Another mesh, the diamond mesh, can be associated to the DDFV structure. This third mesh is very convenient when we have to implement the DDFV method because it is a link between primal and dual meshes in which they both play a symmetric role. In particular, this is on the diamond mesh that we define the discretized gradient. To create the diamond mesh, we construct quadrangle associated to each edge of the primal and dual mesh like in Fig. 1.

2.2 Time Discretization

The transport equation on a bounded open set $\Omega \subset \mathbb{R}^2$, with a divergence-free velocity u , can be written as:

$$\frac{d\phi}{dt} = -\text{div}(\phi u) := \mathcal{L}(\phi) \quad (1)$$

For the time discretization, we follow [5] and use a TVD Runge-Kutta of order k . The order k is then chosen to be in adequation with the order of the spatial discretization, that means here $k = 2$. Let Δt be the time step of the method, we will denote by ϕ^n the approximation of function ϕ at time $t_n = n \Delta t$. The RK2 scheme is then given by the following steps:

$$\phi^{n,1} := \phi^n + \Delta t \mathcal{L}(\phi^n), \quad \phi^{n+1} := \frac{1}{2}\phi^n + \frac{1}{2}\phi^{n,1} + \frac{1}{2}\Delta t \mathcal{L}(\phi^{n,1}) \quad (2)$$

We will now focus on the space discretization of operator \mathcal{L} by a WENO method.

2.3 Discretization of Operator $\text{div}(\phi U)$

Let $\phi^\tau = (\phi_C)_{C \in \mathfrak{M} \cup \mathfrak{M}^*}$, the vector of the approximations ϕ_C of the mean values $\bar{\phi}_C = \frac{1}{|C|} \int_C \phi$ of function ϕ on the cells $C \in \mathfrak{M} \cup \mathfrak{M}^*$ that we want to compute.

Following the Finite Volume strategy, we integrate the operator \mathcal{L} on each cell:

$$\frac{1}{|C|} \int_C \mathcal{L}(\phi) = \frac{1}{|C|} \int_{\partial C} \phi u \cdot n \quad (3)$$

where n is the outer unit normal to the boundary ∂C of C .

Because the cells are polygonal, we can rewrite the boundary integral as a sum over the edges:

$$\int_{\partial C} \phi u \cdot n = \sum_{\sigma \subset \partial C} \int_{\sigma} \phi u \cdot n_{\sigma} \quad (4)$$

The line integral of the right member can be approximated using a p point Gaussian quadrature. Taking $p = 1$ allows us to find back the classical DDFV formulation of divergence operator. Of course the same work can be done for $p > 1$

$$\int_{\partial C} \phi u.n \approx \sum_{\sigma \subset \partial C} |\sigma| \phi(x_\sigma) u(x_\sigma).n_\sigma \text{ where } x_\sigma \text{ is the middle of } \sigma \quad (5)$$

The WENO scheme consists in approximating for each cell C and each edge σ , the value $\phi(x_\sigma)$ by a convex combination of the value in x_σ of several polynomials whose mean values coincide with the mean values of ϕ on a set of selected cells. This set of cells is called the stencil of the method. The WENO procedure for polynomial reconstructions will be developed in Sect. 3. For the moment, let us assume that we dispose of such an approximation $\phi_{C,\sigma}$. Then we define the spatial discretization \mathcal{L}_C of operator \mathcal{L} using an upwind flux as:

$$\begin{aligned} \mathcal{L}_C(\phi^\tau) := & - \sum_{\sigma=C \cap \tilde{C}} |\sigma| [\phi_{C,\sigma}(u(x_\sigma).n_\sigma)^+ - \phi_{\tilde{C},\sigma}(u(x_\sigma).n_\sigma)^-] \\ & - \sum_{\sigma \in C \cap \partial \Omega} |\sigma| [\phi_{C,\sigma}(u(x_\sigma).n_\sigma)^+ - \phi_b(x_\sigma)(u(x_\sigma).n_\sigma)^-] \end{aligned} \quad (6)$$

where \tilde{C} and C share the edge σ and ϕ_b prescribed through the boundary condition.

Let define $\phi^{n,\tau} = (\phi_C^n)_{C \in \mathfrak{M} \cup \mathfrak{M}^*}$ the vector of the approximation ϕ_C^n of the mean value of ϕ on the cells C at time t_n . The full discretization is then given by:

$$\phi_C^{n+1} := \phi_C^n + \frac{1}{2} \Delta t \left[\mathcal{L}(\phi_C^n) + \mathcal{L}(\phi_C^n + \Delta t \mathcal{L}(\phi_C^n)) \right] \quad (7)$$

The previous work is done in the same way on both primal mesh and dual mesh. If we take a look at Eq. (6), we can see that each cell is only linked with its neighbours. One can then think that primal and dual meshes are totally decoupled. In fact the coupling between the two meshes will be ensured by the reconstruction process as we are going to see in the next section and depends on the degree of the polynomial approximation.

3 Reconstruction Procedure

3.1 Problem Statement

Given a cell C and an edge σ , we want to reconstruct an approximation of $\phi(x_\sigma)$ though we only know the mean values $(\bar{\phi}_C)$ of ϕ on $\mathfrak{M} \cup \mathfrak{M}^*$. Following the WENO strategy, the approximation $\phi_{C,\sigma}$ is computed as a convex combination of several polynomial interpolations of ϕ .

To find those polynomial interpolations, we fix a subset $S \subset \mathfrak{M} \cup \mathfrak{M}^*$, depending on C and σ , and we choose the polynomial $P_S[\phi]$ among the polynomials of degree k as the solution of the following problem:

$$\frac{1}{|C|} \int_C P_S[\phi] = \bar{\phi}_C, \quad \forall C \in S \quad (8)$$

The degree k of polynomial P_S is fixed arbitrary and impacts the size of the stencil S .

For high degree k , interpolation often leads to oscillating polynomials. That is the reason why we compute a convex combination of several different interpolations of ϕ . The weights in the convex combination are chosen in order to favour non-oscillating polynomials

$$\phi_{C,\sigma} = \sum_S a_S P_S[\phi](x_\sigma) \quad (9)$$

In this paper, we choose to focus on the oscillating criterion proposed by Abgrall in [1] but other criterion and weights can be found in [5, 10]:

$$a_S = \frac{(\varepsilon + c_0(P_S[\phi]))^{-4}}{\sum_T (\varepsilon + c_0(P_T[\phi]))^{-4}}, \quad \text{with } c_0(P) = \sum_{|\alpha|=m} |p_\alpha| \text{ for } P = \sum_{|\alpha| \leq m} p_\alpha X^\alpha \quad (10)$$

3.2 Polynomial Interpolation Procedure

Let us consider a stencil $S = \{C_0, \dots, C_l\}$ and $(\bar{\phi}_{C_i})_{i=1..l}$ the mean values of ϕ on the cells C_i . We want to find a polynomial P_S that depends on the stencil S and such as: $\langle P_S \rangle_C = \bar{\phi}_C$, for each $C \in S$. With idea of computing an approximation P_S on the stencil S and to avoid spatial dependency, we use a barycentric representation with respect to a given cell C_0 :

$$P_S = \sum_{|\alpha| \leq n} p_\alpha (X - x_{C_0})^\alpha$$

where x_{C_0} is the barycenter of cell $C_0 \subset S$. When we rewrite the previous equations on P_S in an extended form

$$\sum_{|\alpha| \leq n} p_\alpha \langle (X - x_{C_0})^\alpha \rangle_C = \phi_C, \quad \text{for each } C \in S$$

we can easily see that we have to solve a linear problem $\mathcal{A}X = b$, with $\mathcal{A}_{K,\alpha} = \langle (X - x_{C_0})^\alpha \rangle_C$, $X = (p_\alpha)_\alpha$ and $b = (\bar{\phi}_C)_{C \in S}$. If the matrix \mathcal{A} is invertible, the stencil S is called admissible. In practice, we don't have access to an easy way to know if a stencil is admissible. When a stencil is not admissible, then we have to change

the stencil, test again if it is admissible and repeat those operations until we find an admissible one.

3.3 Stencil Choice

The choice of the stencil is a crucial point in the construction of the scheme. Stencils will be composed of both primal and dual cells. As in classical WENO scheme stencils have to be centered in the smooth regions and one-sided near the shocks.

The usual strategy is to associate a given number of stencil to each cell, and then to evaluate the corresponding polynomials on each edges. Here, because the natural structure to use in DDFV schemes is the diamonds structure, we define stencils from this structure. We associate stencils to each couple (C, σ) and each couple is associated to an unique diamond \mathcal{D} , see Fig. 2 (left). Let us define $\mathcal{V}(\mathcal{D}) = \{\mathcal{D}' / \text{such that } \mathcal{D} \cap \mathcal{D}' \neq \emptyset\}$. In order to construct the stencils, we will use the unknowns provided by \mathcal{D} but also by $\mathcal{V}(\mathcal{D})$ and $\mathcal{V}(\mathcal{V}(\mathcal{D}))$. This choice allows us to have access to enough unknowns on the boundary and to construct centered as one-sided stencils.

Then we will construct the stencils associated to (C, σ) as follows. First, we set C as the first cell of the stencil. Then we will choose randomly the other ones (if needed) in $\mathcal{D} \cup \mathcal{V}(\mathcal{D}) \cup \mathcal{V}(\mathcal{V}(\mathcal{D}))$.

Because diamonds are quadrangles and two neighbours share an edge, the number \mathcal{N}_u of potential unknowns is then given by $\mathcal{N}_u \leq 4 + 4 \times 2 + 3 \times 4 \times 2 = 36$.

For a reconstruction of order 0, we only need one point in the stencil and so we only have one potential stencil. One can easily see that in that case we find back the classical upwind scheme and both primal and dual meshes are totally decoupled. For a reconstruction of order greater than 0, primal and dual mesh are coupled. For example in the case of order 2, we have at most $\mathcal{N}_S = \binom{36}{5}$ different stencils. We can however mention that in practice, the maximal number of potential unknowns is not achieved (see Fig. 2 for examples).

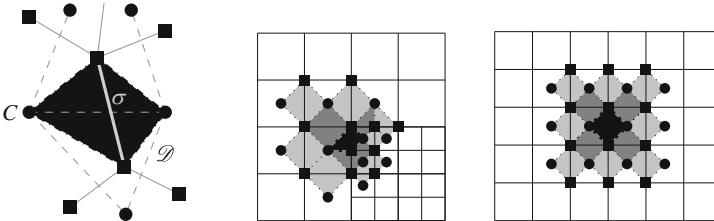


Fig. 2 Diamond cells. \mathcal{D} is in black, $\mathcal{V}(\mathcal{D})$ in gray and $\mathcal{V}(\mathcal{V}(\mathcal{D}))$ in light gray

4 Numerical Tests

In all the following tests, we use a locally refined mesh like in Fig. 1. The previous WENO scheme is implemented in each case with 15 stencils.

4.1 Sinus Translation

First, we test our WENO scheme on the equation

$$\frac{\partial \phi}{\partial t} + \frac{\partial \phi}{\partial x} + \frac{\partial \phi}{\partial y} = 0, \quad (x, y) \in [-2; 2] \times [-2; 2]$$

with the initial condition $\phi_0(x, y) = \sin(\frac{\pi}{2}(x + y))$. One can refer to [10] for comparison of the results. Tests are done with a time step equal to $\Delta t = 0.01$ and in each case we compute the L_1 error at time $t = 2$. The results for the error and the order of the scheme are presented in Table 1 (mesh size refers for the minimal size of the square cells). We obtain an order 2 for the method, which is in adequation with the degree of the polynomial reconstruction.

4.2 Solid Body Rotation (SBR)

Solid body rotation is a classical test used in the literature for advection equation. Zalesak proposed in [14] the rotation of a slotted cylinder. The width of the slot as well as the “bridge” connecting the two half must be about 5 cells. Here, we choose an adaptation of this test introduced in [12] and used in [2]. It consists in the rotation of three body shapes, a hump, a cone and a the slotted cylinder of Zalesak. The overvalue of the initial condition is given on Fig. 3 (left). We choose $\Delta t = 0.005$ and a mesh size $h = 1/128$. As it is mention in [2], a way to measure the accuracy of the scheme is to count the number of isolines outside of the slot. Figure 3, show the isolines at $t = 2\pi$. We can see here that all the isolines fit the slot. Results at $t = \pi$ in Fig. 3 are here to point the fact that all three shapes really pass through the refined part of the mesh.

Table 1 L_1 error for sinus translation

Mesh size	$1.25 \cdot 10^{-1}$	$6.25 \cdot 10^{-2}$	$3.125 \cdot 10^{-2}$	$1.5625 \cdot 10^{-2}$
Error L_1	$5.699 \cdot 10^{-1}$	$1.448 \cdot 10^{-1}$	$3.363 \cdot 10^{-2}$	$7.884 \cdot 10^{-3}$
Order	—	1.98	2.10	2.09

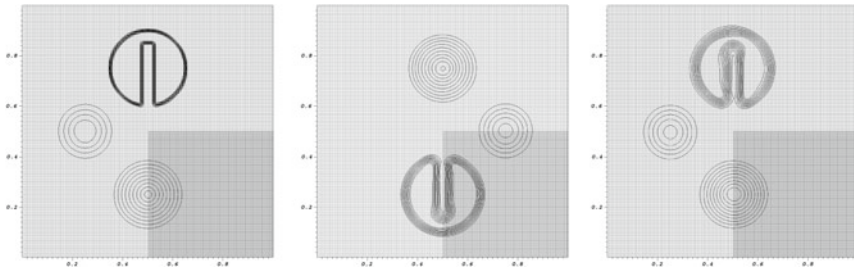


Fig. 3 Isovalues from 0.1 to 0.9 for SBR. From the *left* to the *right* Isovalues at $t = 0, \pi, 2\pi$

5 Conclusion

We presented in this paper a DDFV approach for WENO scheme working on any structured and unstructured grids. We exhibited the expected order 2 of the scheme on smooth test case. The experiment on the SBR test seems also very promising. This approach will have many applications in moving domains on adaptative meshes.

References

1. Abgrall, R.: On essentially non-oscillatory schemes on unstructured meshes: analysis and implementation. *J. Comput. Phys.* **114**(1), 45–58 (1994)
2. Clain, S., Diot, S., Loubère, R.: A high-order finite volume method for hyperbolic systems: Multi-dimensional Optimal Order Detection (MOOD). *J. Comput. Phys.* pp. 0–0 (2011)
3. Domelevo, Komla, Omnes, Pascal: A finite volume method for the laplace equation on almost arbitrary two-dimensional grids. *ESAIM: Math. Model. Numer. Anal. (Modlisation Mathématique et Analyse Numérique)* **39**(6), 1203–1249 (2005)
4. Eymard, R., Gallout, T., Herbin, R.: Finite volume methods. In: *Solution of Equation in n (Part 3), Techniques of Scientific Computing (Part 3), Handbook of Numerical Analysis*, vol. 7, pp. 713–1018. Elsevier (2000). [http://dx.doi.org/10.1016/S1570-8659\(00\)07005-8](http://dx.doi.org/10.1016/S1570-8659(00)07005-8). <http://www.sciencedirect.com/science/article/pii/S1570865900070058>
5. Friedrich, O.: Weighted essentially non-oscillatory schemes for the interpolation of mean values on unstructured grids. *J. Comput. Phys.* **144**(1), 194–212 (1998)
6. Harten, A., Engquist, B., Osher, S., Chakravarthy, S.R.: Uniformly high order accurate essentially non-oscillatory schemes, iii. *J. Comput. Phys.* **131**(1), 3–47 (1997)
7. Harten, A., Osher, S.: Uniformly high-order accurate nonoscillatory schemes. I. *SIAM J. Numer. Anal.* **24**(2), 279–309 (1987). doi:[10.1137/0724022](https://doi.org/10.1137/0724022)
8. Harten, A., Osher, S., Engquist, B., Chakravarthy, S.R.: Some results on uniformly high-order accurate essentially nonoscillatory schemes. *Appl. Numer. Math.* **2**(3), 347–377 (1986)
9. Hermeline, F.: A finite volume method for the approximation of diffusion operators on distorted meshes. *J. Comput. Phys.* **160**(2), 481–499 (2000)
10. Hu, C., Shu, C.W.: Weighted essentially non-oscillatory schemes on triangular meshes. *J. Comput. Phys.* **150**(1), 97–127 (1999)
11. Krell, S.: Schémas volumes finis en mécanique des fluides complexes. Ph.D. thesis, Aix-Marseille Université (2010)
12. LeVeque, R.J.: High-resolution conservative algorithms for advection in incompressible flow. *SIAM J. Numer. Anal.* **33**(2), 627–665 (1996)

13. Shu, C.W., Osher, S.: Efficient implementation of essentially non-oscillatory shock-capturing schemes. *J. Comput. Phys.* **77**(2), 439–471 (1988)
14. Zalesak, S.T.: Fully multidimensional flux-corrected transport algorithms for fluids. *J. Comput. Phys.* **31**(3), 335–362 (1979)

Finite Volumes for Complex Applications VIII - Hyperbolic,
Elliptic and Parabolic Problems

FVCA 8, Lille, France, June 2017

Cancès, C.; Omnes, P. (Eds.)

2017, XV, 559 p. 167 illus., 149 illus. in color.,

Hardcover

ISBN: 978-3-319-57393-9